Ioannis Pytharoulis, Ph.D.
Aristotle University of Thessaloniki
pyth@geo.auth.gr

Numerical Study on the Influence of Surface Conditions on an Intense Storm over Northern Greece

The sea surface temperatures may influence the atmosphere in different ways. Nowadays, various datasets are available for the definition of this field in the numerical weather prediction models. An intense storm associated with heavy precipitation, floods and lightning activity, affected northern Greece on 15 July 2014. The aim of this study was to investigate the influence of the sea surface temperatures on this high impact event. High-resolution numerical experiments were performed with the use of the Weather Research and Forecasting (WRF) numerical weather prediction model. The potential for lightning activity was estimated diagnostically by the Lightning Potential Index. The sensitivity experiments were forced by the sea surface temperature datasets of the National Centers for Environmental Prediction (NCEP), the European Centre for Medium-Range Weather Forecasts (ECMWF) and the National Aeronautics and Space Administration (NASA), which exhibited differences up to about 1°-2°C. The surface fluxes of energy were modulated by the above datasets. The sea surface temperatures appeared to affect the spatial distribution of precipitation and the spatiotemporal distribution of the lightning activity. The existence of actual sea surface temperature measurements is deemed necessary in order to reduce the uncertainty in the definition of the surface conditions in the numerical weather forecasts.
Keywords: intense precipitation, sea surface temperatures, WRF model, Lightning Potential Index, neighbourhood based verification

Introduction

Various studies have shown the importance of the surface conditions for meteorology and climate (e.g. Garratt, 1993). The sea surface temperatures (SSTs) may control the evolution of the weather systems at different scales. High impact weather events in the Mediterranean, such as torrential precipitation, floods, tornadoes and tropical-like cyclones, have been affected by the SSTs (e.g. Miglietta et al., 2011, 2017; Millan et al., 1995; Pytharoulis, 2017). Tompkins and Craig (1999) suggested that the SST changes influence convection, only in the presence of large scale flow. However, the explosive deepening of the eastern Meditteranean "bomb" of January 2004 was not sensitive to the surface fluxes and the SSTs (Lagouvardos et al., 2007; Katsafados et al., 2011). The latter authors suggested that only the spatial distribution of precipitation was sensitive to the definition of the SSTs (satellite/ analysis data). Also, a numerical study of the Mediterranean tropical-like cyclone of November 2014 simulated a slightly weaker system when warm SST anomalies of 2°C and 3°C were imposed (Pytharoulis, 2017), because of changes in its upper air warm core. Therefore, the SSTs may influence the atmosphere in different ways. This is particularly important in numerical weather prediction because miscellaneous SST datasets, produced by different techniques and at various resolutions, are available.

An intense storm (with strong precipitation and lightning activity) occurred at northern Greece, and mainly in the Gulf of Thermaikos, in Thessaloniki, as well as in western Chalkidiki, on 15 July 2014. The precipitation reached 98.5 mm and 61 mm at the meteorological station

of the Aristotle University of Thessaloniki (AUTH) and at the city airport in a 24 hr interval ending at 18:00 UTC 15/7/14. Its development was associated with a mid-tropospheric closed low and strong low-level convergence, in an environment supporting deep convection. Pytharoulis et al. (2016) presented a detailed synoptic/dynamic analysis of the event and showed the important role of the strong synoptic forcing. Tolika et al. (2017) proposed that a "lake" effect, due to SST warming in the almost closed Gulf of Thessaloniki, is likely to have promoted this event. The aim of the present study is to investigate the influence of the SSTs on the development of this event, which affected a highly populated area and tourist destination, focusing on precipitation and lightning activity.

Data and methodology

This study utilizes surface observations from the meteorological stations of the Department of Meteorology and Climatology in AUTH and the airport of Thessaloniki (LGTS; Figure 1). The precipitation was also estimated from the weather radar of the 3D S.A. company at Filyro (40.672°N, 23.014°E), using the TITAN software. This radar is used operationally by the Hellenic Agricultural Insurance Organization in its hail suppression activities in northern Greece. The lightning data were measured by the ZEUS system (Kotroni & Lagouvardos, 2008, 2016; Lagouvardos et al., 2009) operated by the National Observatory of Athens.

The numerical experiments were performed using the non-hydrostatic Weather Research and Forecasting (WRF) numerical weather prediction model, with the Advanced Research dynamic core (WRF-ARW version 3.5.1; Skamarock et al., 2008; Wang et al., 2013). Figure 1 shows that two model domains were applied (a) in Balkans, southern Italy and in a part of the eastern Mediterranean Sea (D01; 292 x 288 grid points) and (b) in the wider area of northern Greece (D02; 219 x 171 grid points). The horizontal grid-spacing of the two-way nested domains D01 and D02 was 5 km and 1.667 km, respectively, while 51 sigma levels (up to 50 hPa) were used in the vertical by both nests. The initial and boundary conditions of D01 were based on the 6 hourly operational analyses of the European Centre of Medium-Range Weather Forecasts (0.125°x0.125° latitude-longitude). High-resolution (30 arc sec) data from the United States Geological Survey, were used in order to define the topography and the land use.

The microphysical, boundary layer, surface layer and soil processes were modeled by the WRF Single-Moment 6-Class (WSM6; Hong & Lim, 2006), Yonsei University (YSU; Hong et al., 2006), Monin-Obukhov (MM5), NCEP/ Oregon State University / Air Force/ Hydrologic Research Lab (NOAH; Chen & Dudhia, 2001) schemes, respectively. NOAH used four layers extending at 0-0.1, 0.1-0.4, 0.44-1.0 and 1.0-2.0 m below the surface. The cumulus convection was parameterized at D01 using the Kain-Fritsch scheme (Kain, 2004), while it was considered to be explicitly resolved in the inner nest (D02), due to its fine resolution. The shortwave and longwave radiation fluxes were represented by the RRTMG scheme (rapid radiative transfer model application for global climate models; Iacono et al., 2008), taking into account the terrain slope in the calculation of the former fluxes. This model setup was used successfully by Pytharoulis et al. (2016) in a numerical study of the effect of topography on this event.

The sensitivity of the intense precipitation event of 15 July 2014 and its lightning activity on the SSTs was investigated through the implementation of three numerical experiments, with:

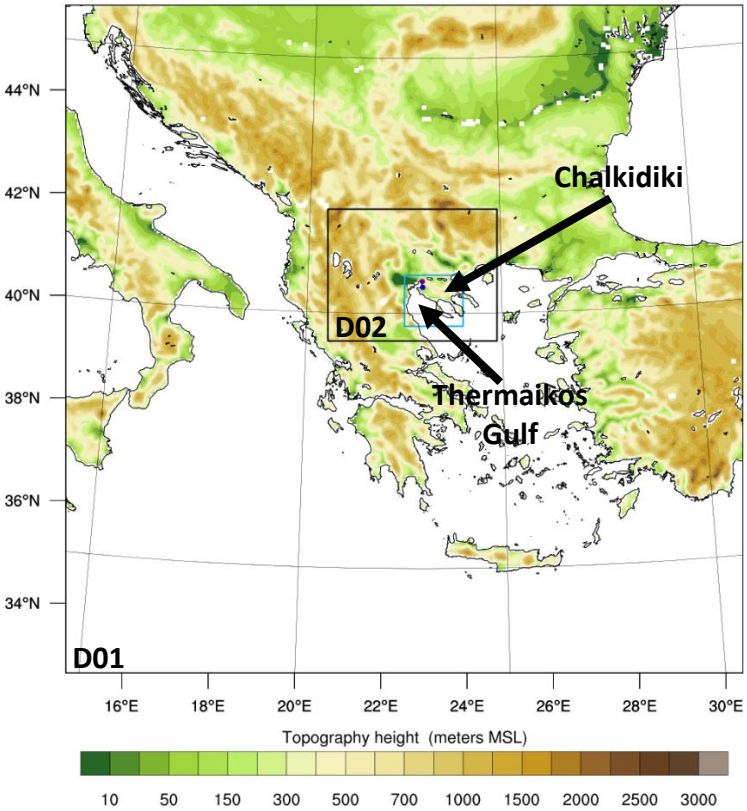

Figure 1 The two domains (D01, D02) used in the numerical experiments of WRF-ARW model. The colour shading illustrates the topography of D01. The blue rectangle encompasses the region of interest (39.75°N – 40.75°N, 22.5°E - 24°E). The locations of the meteorological stations of the Aristotle University of Thessaloniki (AUTH) and the airport of Thessaloniki (LGTS) are depicted by the magenta and blue colored bullets, respectively.

(a) The daily high-resolution SSTs of the National Centers for Environmental Predictions (NCEP) at a grid-spacing of 1/12° x 1/12° (~0.083°x0.083°) latitude-longitude (http://polar.ncep.noaa.gov/sst/ophi/; hereafter NCEP_SST or control experiment).
(b) The SSTs of the 6-hourly ECMWF analyses at a grid-spacing of 0.125°x0.125° (ECMWF_SST).
(c) The daily National Aeronautics and Space Administration / Jet Propulsion Laboratory (NASA/JPL) SSTs, at a grid-spacing of 0.01°x0.01° latitude-longitude (Chao et al., 2009), which are produced through multi-sensor satellite data and in situ buoy observations (NASA_SST).
All the experiments were performed from 12:00 UTC 14 July 2014 to 18:00 UTC 15 July 2014 and the SSTs did not change relatively to the initial values. The simulated lightning activity was calculated diagnostically through the Lightning Potential Index (LPI; Yair et al., 2010) using the WRF output at 5 minute intervals. The selected WSM6 microphysical scheme is suitable for such applications, because it is effective in high resolution simulations and computes the mass mixing ratio of liquid water, graupel, snow and ice which are needed by LPI.

Results

Figure 2 illustrates the SSTs of the three experiments in the inner domain (D02). In NCEP_SST, the surface temperatures ranged from about 24.5°C to 25.5°C at the Gulf of Thermaikos. The

SSTs of ECMWF_SST were generally warmer than NCEP SSTs, up to about 1-1.5°C, in the Gulf of Thermaikos where heavy precipitation was estimated (Figure 3a) and most of the lightning activity took place. Similarly, the NASA SSTs were warmer than in the control experiment, with anomalies up to about 1.5-2°C. Moreover, the higher resolution SSTs of NASA were able to resolve smaller scale anomalies, especially near AUTH and LGTS.

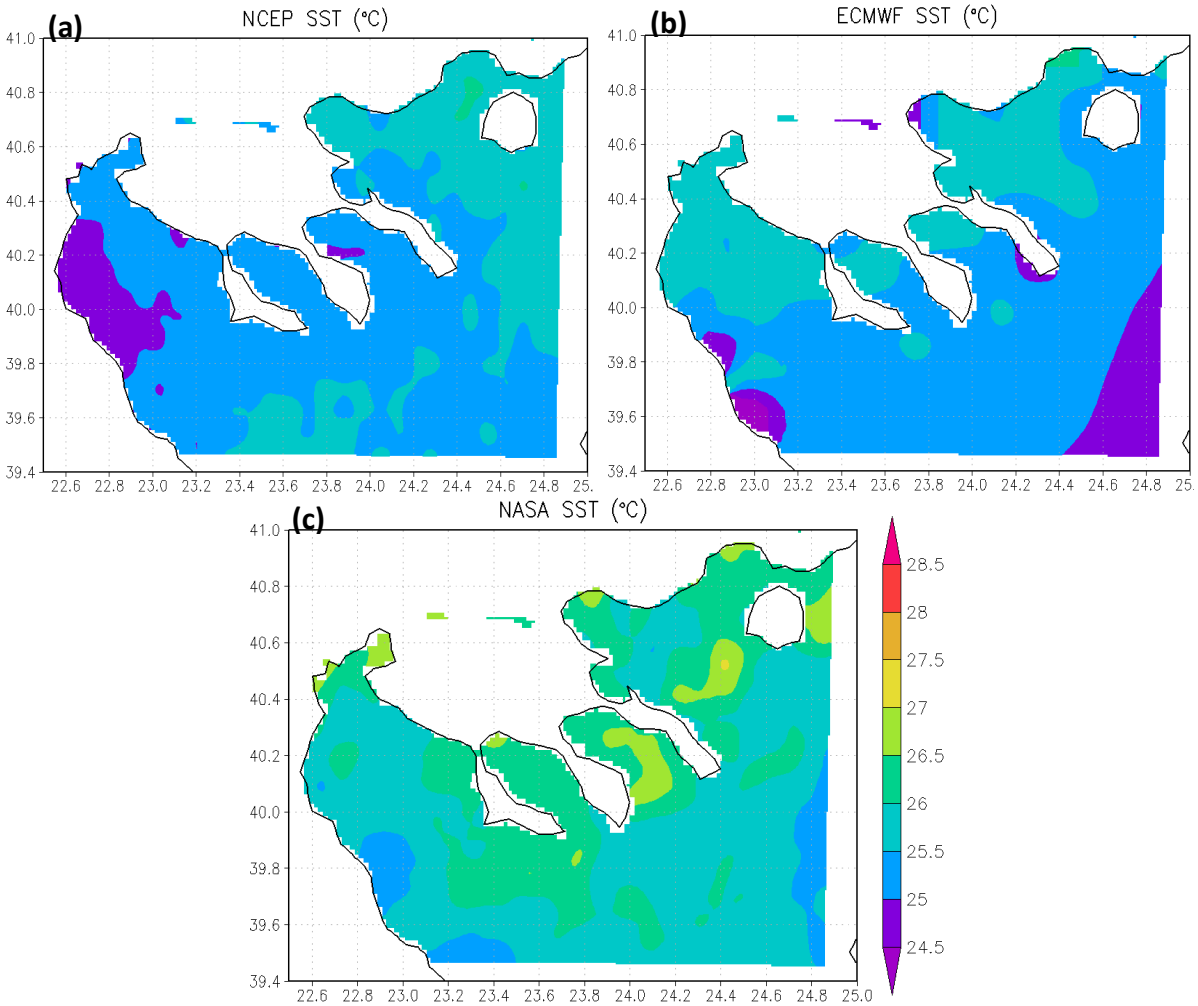

Figure 2 The sea-surface temperatures (°C) of D02, in the (a) NCEP_SST, (b) ECMWF_SST and (c) NASA_SST WRF experiments.

The accumulated precipitation estimated by the C-band weather radar from 18 UTC 14/7/14 to 18 UTC 15/7/14, at a radius of 100 km, appears in Figure 3a. The 24 hr precipitation exceeded 40 mm (and even 90 mm locally) in large parts of western Chalkidiki and Thessaloniki where the floods occurred. In agreement with the radar data, all the experiments simulated large precipitation amounts greater than 40 mm in the abovementioned areas, near AUTH and LGTS where the maximum amounts were recorded, and in the Gulf of Thermaikos (Figure 3). The heaviest precipitation (> 100 mm in 24 hr in Thermaikos Gulf and western Chalkidiki) was simulated by NASA_SST (Figure 3d), that was forced by the warmest SSTs (Figure 2).
High resolution simulations may provide a realistic representation of the atmospheric flow, but, they may suffer from displacement errors (Ebert, 2008). AUTH measured 98.5 mm in the aforementioned 24 hr period. The maximum 24 hr precipitation near AUTH was simulated at about 24.2 km, 24.6 km, 13.2 km southeast of the station, with amounts of 94 mm, 85.6 mm and 85 mm in NCEP_SST, ECMWF_SST and NASA_SST, respectively. Hence, the statistical

evaluation of the simulated precipitation against the radar-derived one was performed using the neighborhood based methodology of Clark et al. (2010). Firstly, the radar values were interpolated to the grid of D02. Then, they were compared with the simulated values at neighborhoods of different sizes, instead of using a point-to-point evaluation. The cone of silence and the region southeast of the radar, influenced by the mountains and technical issues, were not considered. The neighborhoods corresponded to squares centered at each grid-point, with their sides extending progressively from about 3.33 km x 3.33 km to 100 km x 100 km. Following Clark et al. (2010), at a specific precipitation threshold, a hit is counted at a grid-point when the observed value exceeds it at this grid-point and the simulated value exceeds it at the same grid-point or at least at one grid-point of the neighborhood.

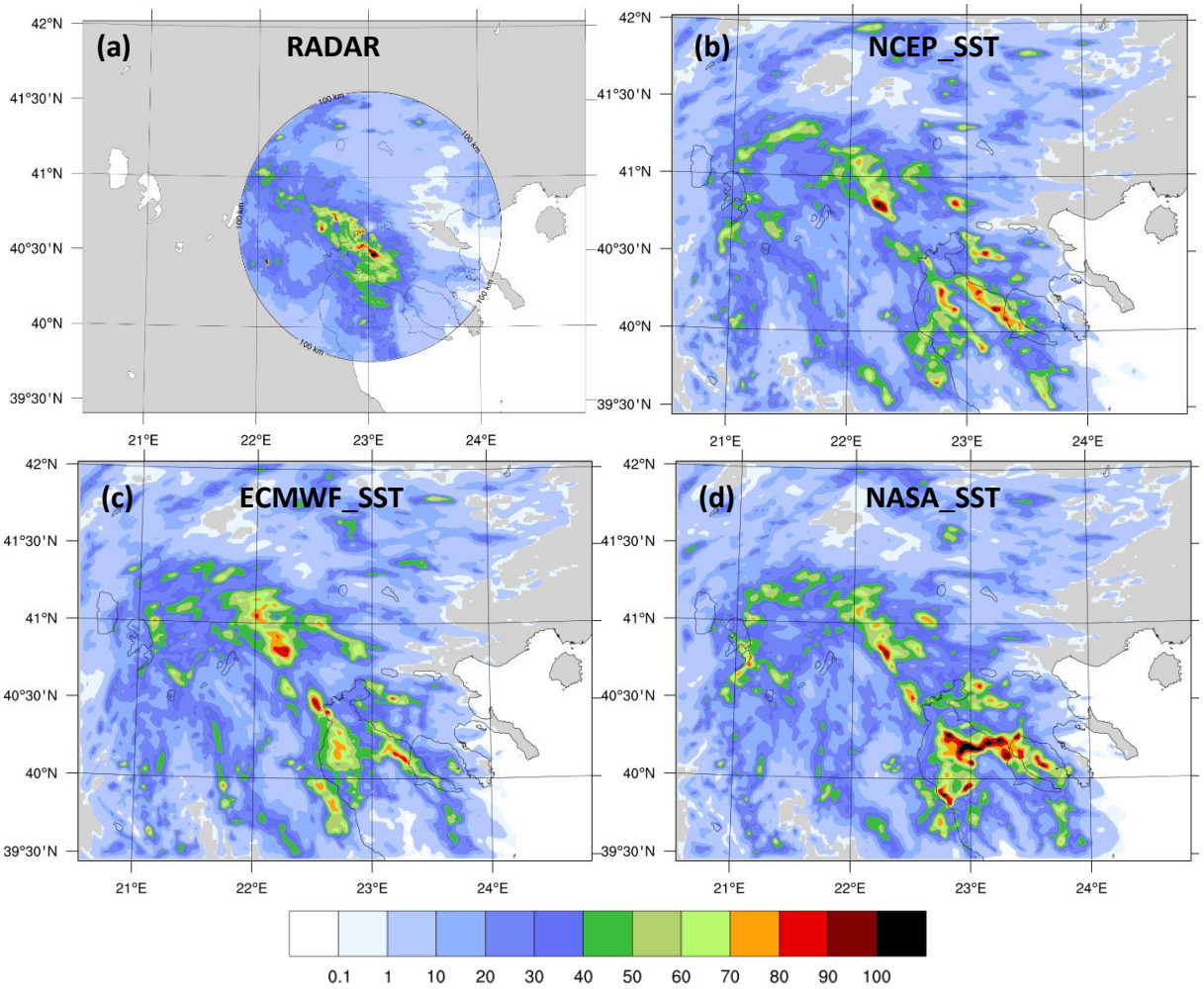

Figure 3 The accumulated precipitation (mm) (a) estimated by the weather radar and simulated by the WRF-ARW experiments (b) NCEP_SST, (c) ECMWF_SST and (d) NASA_SST in D02, from 18:00 UTC 14/7/2014 to 18:00 UTC 15/7/2014.

The statistical scores were calculated for each different size of neighborhoods using the Model Evaluation Tool (MET) of WRF. Figure 4 shows the maximum value of the Equitable Threat Score (ETS) in the different size neighborhoods versus the precipitation threshold. The ECMWF_SST (NCEP_SST) produced the best spatial distribution of the 24 hr precipitation for thresholds larger (smaller) than 45 mm. The NASA_SST exhibited higher scores than NCEP_SST only for large thresholds greater than 55 mm in 24 hr.

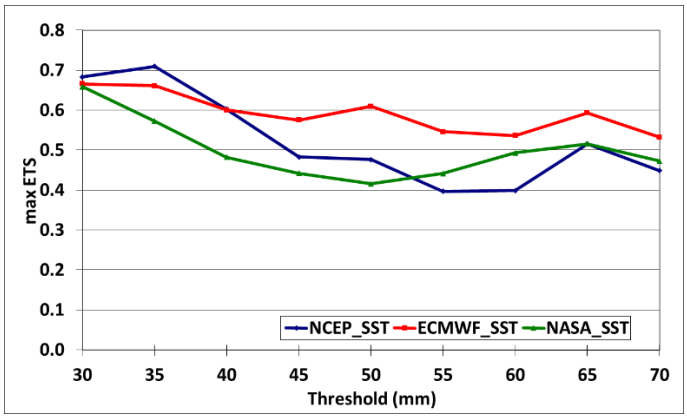

Figure 4 The maximum Equitable Threat Score (ETS) of the D02 precipitation accumulated from 18UTC 14/7/14 to 18UTC 15/7/14, for neighborhood sizes up to 100 km x 100 km, versus the precipitation threshold (mm) in NCEP_SST, ECMWF_SST and NASA_SST experiments.

The horizontal distribution of the density of lightning strikes at the grid-points of D02, from 18 UTC 14/7/14 to 18 UTC 15/7/14, is illustrated in Figure 5a. Most of the lightning activity affected the Gulf of Thermaikos, the two western peninsulas of Chalkidiki (Kassandra and Sithonia) and the region near the city and the airport of Thessaloniki. All the experiments simulated the threat in these regions, through the LPI index (Figure 5). The maximum predicted values appeared in the Gulf of Thermaikos, near the western peninsula of Chalkidiki (Kassandra) and near the northwest borders of Greece. The overestimation of the latter activity is likely to be due to model errors and to the complexity of processes involved in lightning physics. The NASA_SST experiment provided the most pronounced indication of the lightning threat in the above regions and mainly at Thessaloniki.

Figure 6 presents the temporal evolution of the actual and simulated lightning activity in the area of interest (39.75°N-40.75°N, 22.5°E-24.0°E; Figure 1) in half-hourly intervals. This rectangle was successfully used by Pytharoulis et al. (2016), in order to examine the effect of topography in this event, and is adopted here. All the experiments simulated most of the duration of the lightning activity. NASA_SST experiment provided the best estimate (a) of the triggering of the activity, but with a delay of about 2 hours and (b) of the time of peak activity. The statistical scores were calculated using the half-hourly number of actual strikes and maximum LPI in the area of interest (39.75°N-40.75°N, 22.5°E-24.0°E) in the whole 24hr period (Figure 6). A hit was considered when the number of the actual strikes and maximum LPI were greater than zero. NASA_SST produced the best temporal distribution of the lightning activity. NCEP_SST and ECMWF_SST exhibited identical scores, but the latter experiment produced a higher linear correlation coefficient (0.597).

The SSTs influence the troposphere through the surface fluxes of heat and moisture. In turn, they change the equivalent potential temperature of the boundary layer, modulating the likelihood and intensity of convection. The warmer SSTs of the NASA dataset resulted to the simulation of the strongest average surface latent heat fluxes (at the sea points of the area of interest) before the triggering and during most of the lifetime of the lightning activity in NASA_SST, followed by ECMWF_SST (Figure 7). The average surface latent heat fluxes in NASA_SST (ECMWF_SST) over the sea points of the area of interest were about 35 W/m^2 (15 W/m^2) stronger than in NCEP_SST at the outset of the lightning activity. The average surface sensible heat fluxes were almost zero before the event, but reached about 30% of the surface latent heat values during the event. Similarly, the strongest sensible heat fluxes were simulated by NASA_SST, followed by ECMWF. Therefore, it seems that the warmer SSTs

resulted to an earlier triggering of the lightning activity in NASA_SST, closer to the observed time of its outset, and an improvement of the temporal correlation between the actual and the simulated activity in NASA_SST and ECMWF_SST (Figure 6).

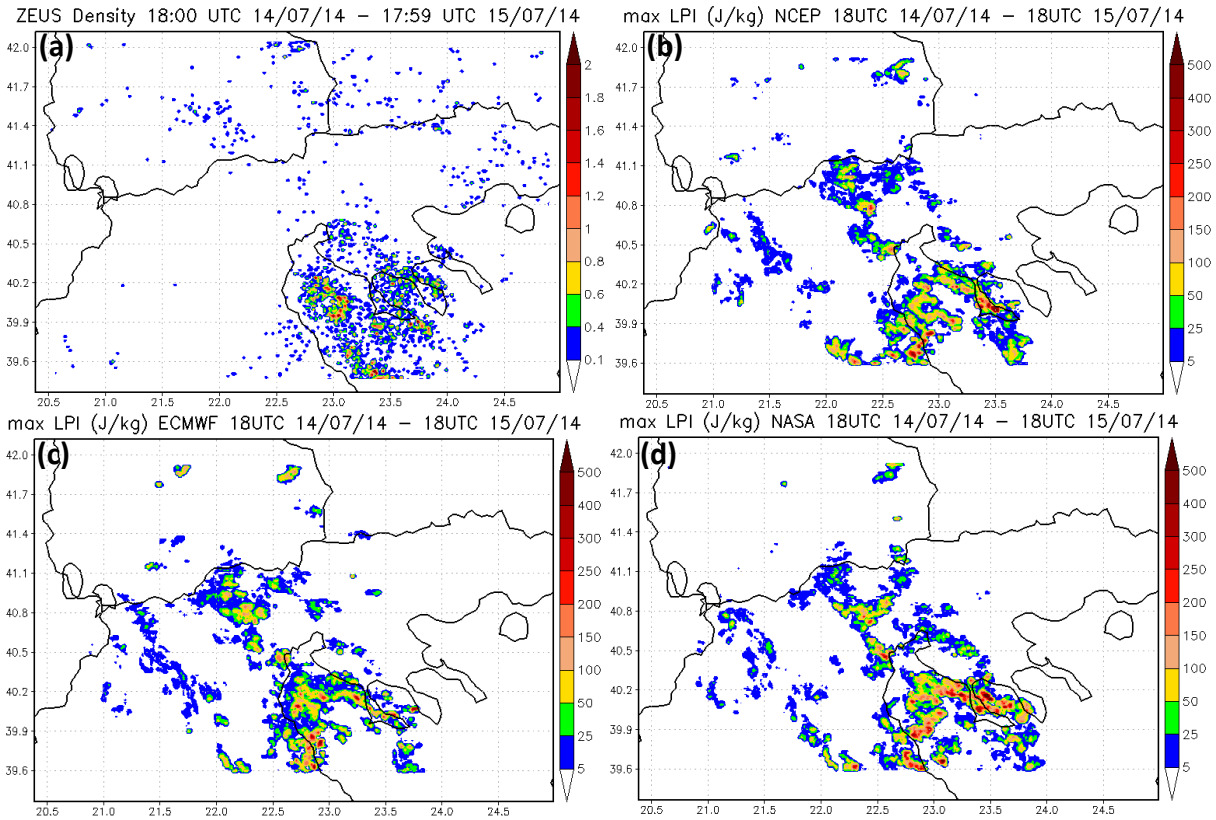

Figure 5 (a) The density of lightning strikes (number/km^2) detected by the ZEUS system and (b), (c), (d) the maximum value of LPI (J/kg) in the NCEP_SST, ECMWF_SST and NASA_SST experiments of WRF-ARW, respectively, in D02 from 18UTC 14/7/14 to 18UTC 15/7/14.

Summary - Conclusions

This study investigated the sensitivity of an intense precipitation and lightning event, which affected northern Greece on 15 July 2014, to the sea surface temperatures. Three high resolution numerical experiments were performed with the use of the non-hydrostatic WRF-ARW model. The simulations were forced by the operational NCEP, ECMWF and NASA/JPL SST datasets which exhibited differences up to about 1°-2°C in the Gulf of Thermaikos. Both ECMWF and NASA SSTs were warmer than the NCEP ones in the Gulf, despite the slightly lower resolution of the ECMWF dataset. All the experiments simulated heavy precipitation, stronger than 40 mm/ 24 hr, in large parts of the affected regions. The maximum simulated values exceeded 80 mm/ 24 hr locally in agreement with the radar data. The statistical evaluation of the model precipitation against the radar estimated one, was performed through a neighbourhood based verification method. It showed that the experiment with the ECMWF SST field, which is created by the same assimilation system as the meteorological input data, resulted to the best representation of the spatial distribution of precipitation. The best representation of the outset and maximum intensity times, as well as of the temporal

evolution of the whole lightning activity were produced by the experiment with the NASA SSTs. It is suggested that the warmer SSTs of NASA improved the representation of the temporal evolution of instability, allowing a more efficient triggering of the lightning activity. In conclusion, this intense event was sensitive to the definition of the sea surface temperatures. Unfortunately, no actual SST measurements are available in this area, resulting to large differences in the various SST datasets. The existence of an observational SST network is deemed necessary in this region.

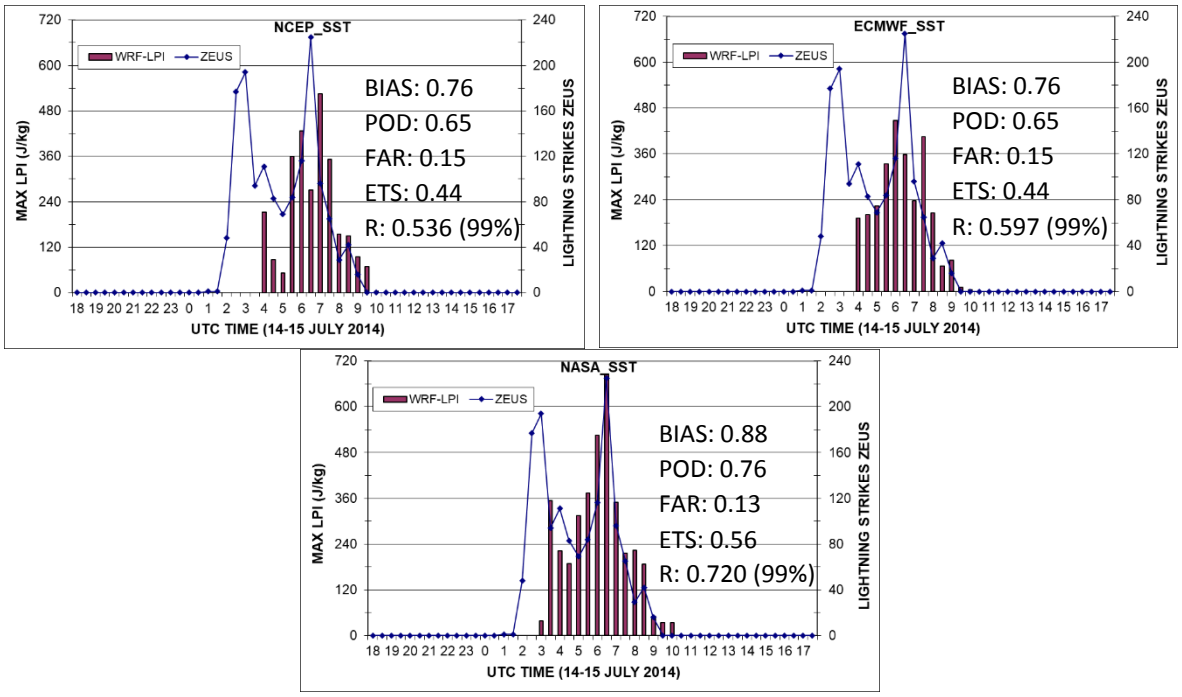

Figure 6 Timeseries of the number of ZEUS lightning strokes and the maximum value of the calculated LPI (J/kg) in half-hourly intervals in the area of interest (39.75°N-40.75°N, 22.5°E-24.0°E). The number of each hour appears at the first half-hourly interval of the hour. The frequency Bias, Probability Of Detection, False Alarm Rate, Equitable Threat Score, linear correlation coefficient (R) and its significance level at each experiment are also provided.

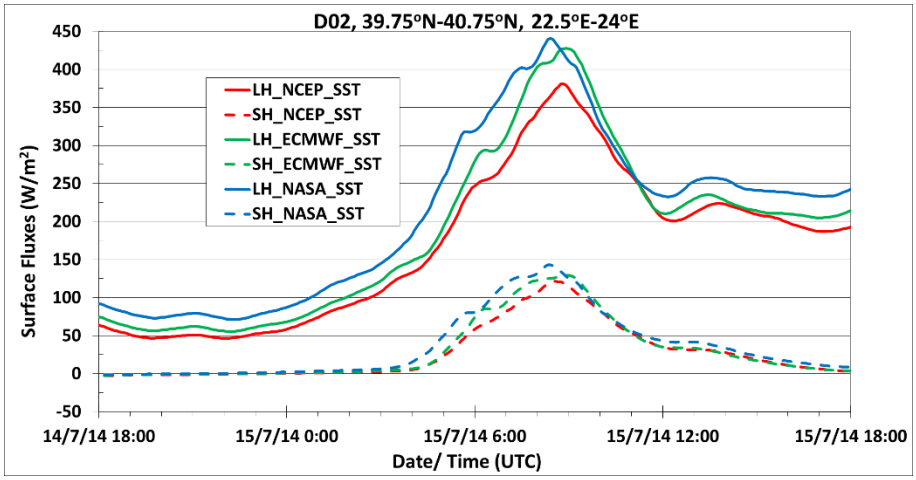

Figure 7 Timeseries of the surface latent (LH) and sensible heat (SH) fluxes averaged over the sea points of the area of interest (39.75°N-40.75°N, 22.5°E-24.0°E) of D02.

References

Chao, Y., Li, Z., Farrara, J. D., & Huang, P. (2009). Blended sea surface temperatures from multiple satellites and in-situ observations for coastal oceans. *Journal of Atmospheric and Oceanic Technology*, 26 (7), 1435-1446.

Chen, F., & Dudhia, J. (2001). Coupling an advanced land-surface/hydrology model with the Penn State/NCAR MM5 modeling system. Part I: Model description and implementation. *Mon. Weather Rev.*, 129, 569–585.

Clark, A. J., Gallus Jr., W. A., & Weisman, M. L. (2010). Neighborhood-based verification of precipitation forecasts from convection-allowing NCAR WRF model simulations and the operational NAM. *Weather Forecast.*, 25, 1495–1509. http://dx.doi.org/10.1175/ 2010WAF2222404.1.

Ebert, E.E. (2008). Fuzzy verification of high-resolution gridded forecasts: a review and proposed framework. *Meteorol. Appl.*, 15, 51-64.

Garratt, J. (1993). Sensitivity of climate simulations to land surface and atmospheric boundary-layer treatments – a review. *Journal of Climate*, 6, 419 – 449.

Hong, S.-Y., & Lim, J.-O.J. (2006). The WRF single-moment 6-class microphysics scheme (WSM6). *J. Korean Meteor. Soc.*, 42, 129–151.

Hong, S.-Y., Noh, Y., & Dudhia, J. (2006). A new vertical diffusion package with an explicit treatment of entrainment processes. *Mon. Weather Rev.*, 134, 2318–2341.

Iacono, M. J., Delamere, J. S., Mlawer, E. J., Shephard, M. W., Clough, S. A., & Collins, W. D. (2008). Radiative forcing by long-lived greenhouse gases: calculations with the AER radiative transfer models. *J. Geophys. Res.*, 113, D13103. http://dx.doi.org/10.1029/ 2008JD009944.

Kain, J. S. (2004). The Kain-Fritsch convective parameterization: an update. *J. Appl. Meteorol.*, 43, 170–181.

Katsafados, P., Mavromatidis, E., Papadopoulos, A., & Pytharoulis, I. (2011). Numerical simulation of a deep Mediterranean storm and its sensitivity on sea surface temperature. *Nat. Hazards Earth Syst. Sci.*, 11, 1233-1246. http://dx.doi.org/10.5194/nhess-11-1233-2011

Kotroni, V., & Lagouvardos, K. (2008). Lightning occurrence in relation with elevation, terrain slope and vegetation cover in the Mediterranean. *J. Geophys. Res.*, 113, D21118.

Kotroni, V., & Lagouvardos, K. (2016). Lightning in the Mediterranean and its relation with sea-surface temperature. *Environ. Res. Lett.*, 11, 034006

Lagouvardos, K., Kotroni, V., & Defer, E. (2007). The 21–22 January 2004 explosive cyclogenesis over the Aegean Sea: Observations and model analysis. *Q. J. R. Meteorol. Soc.*, 133, 1519–1531. http://dx.doi.org/10.1002/qj.121

Lagouvardos, K., Kotroni, V., Betz, H.-D., & Schmidt, K. (2009). A comparison of lightning data provided by ZEUS and LINET networks over Western Europe. *Nat. Hazards Earth Syst. Sci.*, 9, 1713–1717.

Miglietta, M. M., Moscatello, A., Conte, D., Mannarini, G., Lacorata, G., & Rotunno, R. (2011). Numerical analysis of a Mediterranean 'hurricane' over south-eastern Italy: sensitivity experiments to sea surface temperature. *Atmos. Res.*, 101, 412–426. http://dx.doi. org/10.1016/j.atmosres.2011.04.006

Miglietta, M. M., Mazon, J., Motola, V., & Pasini, A. (2017). Effect of a positive Sea Surface Temperature anomaly on a Mediterranean tornadic supercell. *Scientific Reports*, 7, 12828. http://dx.doi.org/10.1038/s41598-017-13170-0

Millan, M., Estrela, M. J., & Caselles, V. (1995). Torrential precipitations on the Spanish east coast: The role of the Mediterranean sea surface temperature. *Atm. Res.*, 36, 1–16.

Pytharoulis, I., Kotsopoulos, S., Tegoulias, I., Kartsios, S., Bampzelis, D., & Karacostas, T. (2016). Numerical modeling of an intense precipitation event and its associated lightning activity over northern Greece. *Atmos. Res.*, 169, 523-538. http://dx.doi.org/10.1016/j.atmosres.2015.06.019

Pytharoulis, I., (2017). Analysis of a Mediterranean tropical-like cyclone and its sensitivity to the sea surface temperatures. *Atmos. Res.*, in press. http://dx.doi.org/10.1016/j.atmosres.2017.08.009

Skamarock, W. C., Klemp, J. B., Dudhia, J., Gill, D. O., Barker, D. M., Duda, M. G., Huang, X. Y., Wang, W., & Powers, J. G. (2008). A Description of the Advanced Research WRF Version 3. NCAR/TN-475+STR. pp. 113.

Tolika, K., Maheras, P., & Anagnostopoulou, C. (2017). The exceptionally wet year of 2014 over Greece: a statistical and synoptical – atmospheric analysis over the region of Thessaloniki. *Theor. Appl. Climatol.*, in press. http://dx.doi.org/10.1007/s00704-017-2131-8

Tompkins, A. M, & Craig, G. C. (1999). Sensitivity of Tropical Convection to Sea Surface Temperature in the Absence of Large-Scale Flow. *J. Climate*, 12, 462-476.

Wang, W., Bruyère, C., Duda, M., Dudhia, J., Gill, D., Kavulich, M., Keene, K., Lin, H.-C., Michalakes, J., Rizvi, S., Zhang, X., Beezley, J., Coen, J., Mandel, J., Chuang, H.-Y., McKee, N., Slovacek, T., & Wolff, J. (2013). ARW Version 3 Modeling System User's Guide. NCAR-MMM 411.

Yair, Y., Lynn, B., Price, C., Kotroni, V., Lagouvardos, K., Morin, E., Mugnai, A., & Llasat, M.d.C. (2010). Predicting the potential for lightning activity in Mediterranean storms based on the WRF model dynamic and microphysical fields. *J. Geophys. Res.*, 115, D04205.

Acknowledgments

I would like to thank the National Observatory of Athens and particularly Dr. V. Kotroni and Dr. K. Lagouvardos for making available the ground based ZEUS network lightning data, as well as S. Kotsopoulos and S. Kartsios from AUTH for helpful information on technical issues. The weather radar data were provided by DAPHNE project. NCEP and NASA/JPL are acknowledged for the sea surface temperature datasets, ECMWF for the gridded analyses and NCAR for the WRF – ARW model and the MET software.